CFD GRID GENERATION AND FLOW ANALYSIS OF A COUNTER ROTATING OPEN ROTOR PROPULSION SYSTEM

Thesis

Presented in Partial Fulfillment of the Requirements for the Graduation with Distinction in the Undergraduate School of Engineering at The Ohio State University

By

Monir Shahriar Farooque

Undergraduate Program in Aeronautical and Astronautical Engineering

The Ohio State University

2010

Thesis Committee:

Dr. Mei Zhuang, Advisor

Dr. Jack McNamara

Abstract

Counter Rotating Open Rotor (CROR) systems promise a light weight, fuel efficient means for propulsion for the aerospace industry. The only drawback is its high level aerodynamic noise, which could be analyzed using Computational Aeroacoustic (CAA) methods such as FW-H or AIBM. However, for a better performing CAA tool, a good CFD model and flow solution is first needed. This study focuses on creating both structured and unstructured meshes for two CROR configurations, one with 12x12 blades count and the other with 12x10 count. Three unstructured CFD mesh domains, with varying domain sizes and differing boundary conditions, were solved in FLUENT for a normal sea-level take-off condition for the CROR, with a flow mach number M = 0.2, and compared to each other to see which one is a better fit for accurate flow solutions with less computation time. The results showed that the most suitable CFD model for aerodynamic noise analyses is the single passage unstructured mesh, with periodic boundary conditions and a domain breadth or radius that is about ten times larger than the mean rotor radius,. Furthermore, the CFD model developed in this study is also perfectly suitable for any further CAA investigation in order to reduce noise of the CROR.

Dedication

This work is dedicated to my mother, my step-father and my wife, whose relentless co-operation helped me focus during the toughest of times in my college career.

Also

I am thankful to my two advisors, Dr. Jack McNamara and Dr. Mei Zhuang, for their utmost confidence in me with a project like this which is important for both lowering the environmental impacts of jet-engines and steps towards a green future of aviation.

Acknowledgements

I want to acknowledge the help and contributions of Zach Webster, Samik Bhattachariya and Krishna Guha Velliyur Ramacha in my mastery of FLUENT and other CFD concepts throughout the course of this work.

Vita

2004 to 2006 …… Department of Aerospace Engineering, RMIT University, Melbourne, Australia.

2007 to present …… Department of Aeronautical and Astronautical Engineering, The Ohio State University.

Fields of Study

Major Field:

Bachelor of Science in Aeronautical and Astronautical Engineering

Table of Contents

List of Tables

List of Figures

I. Introduction

Due to the absence of a perimeter binding structure (a duct or a nacelle), design models for the Contra Rotating Open Rotor (CROR) propulsion systems are found to be light weight, more fuel efficient aircraft propulsion systems than conventional turbofans[1]. The advantage of not having a nacelle is two pronged - first, large diameter propellers could be used to capture more air as its working fluid, hence there is less thrust specific fuel consumption (TSFC). Secondly, the overall reduction of structural weight (due to the absence of nacelles) will allow carrying more passengers or cargo which is also a big financial factor in the commercial airline industry today. However, these open rotor jet engines are particularly noisy ones; the very characteristic of openness that allows fuel efficiency can also allow audible sound waves to radiate unobstructed and reach human years miles apart. In conventional engines, on the other hand, the nacelles act as buffers that hold most of the audible sound disturbances from escaping. This problem alone currently makes the CROR less attractive to the airline operators[2]. The high level undesired noise is prone to cause noise pollution anywhere near it might be adopted as means for aircraft propulsion.

The growing interest in developing an economic and environmentally friendly means for jet propulsion had prompted aerospace researchers to investigate the CROR design in the

last three decades, after it was first introduced by GE in the late 1970s[1]. In 1988, GE successfully flew an open-rotor jet engine on an MD-80 across the Atlantic to the Farnborough air-show in England. This flight demonstrated a fuel savings of more than 30 percent compared to similar sized conventional turbofan engines[2]. However, as the noise problem persisted in the design and with the sudden drop of fuel prices in the early 1990s, GE decided to put a halt on its development prematurely.

The recent economic downturn and soaring oil prices have, once again, brought back the focus onto this class of engines. In order to meet the government's stringent carbon emission levels[3], research activities on the fuel efficient CROR has started to take the center stage in the recent years. As a result, there is a renewed interest in reviving the CROR design and reinvestigate its aeroacoustic noise generation aspects.

As it could be seen from Figure 1, that the open rotor engines consist of two rows of counter rotating propellers of large diameters, which are driven by a smaller sized central gas-turbine core engine.

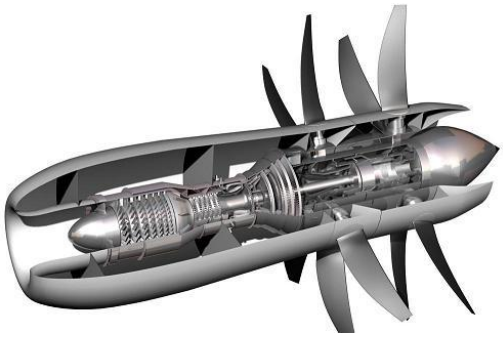

Figure 1: Internal structures of the GE 36 UDF engine[2]

Once in action, the counter rotating propellers create a periodic disturbance in the surrounding flow field, which propagates away from the source in the form of low frequency sound waves. One of the most challenging aspects of the CROR is the tight coupling that exists between the aerodynamics and aeroacoustics properties. Hence, although the open rotors capture a greater flux of incoming air and drive it through the engine exit that increase thrust, they create a great amount of unobstructed noise radiating towards the ground. The situation gets more severe in low flight speeds, such as during takeoffs and landings, when the most noise is generated near ground[1]. Scattering and diffraction of these undesired sound waves by the fuselage and other nearby reflecting surfaces further amplify this effect on the community dwellers and on passengers inside the aircraft[4]. Hence, despite its apparent economic and ecological advantages, the noise of the CROR may cause strong negative public opinion against its wide adoption by passenger careers operating in airports near residential areas.

The focus of the current study is to lay path for a virtual test-bed of CFD based Computational Aero-Acoustics (CAA) models, such as the Ffowcs-Williams and Hawkins method or the AIBM method, that could be used for accurate prediction of pressure perturbation waveforms – which are the primary sources for audible acoustic noise. As it is a matter of great cost, time and effort; wind tunnel tests are not feasible to perform extensive noise reduction research. Hence, in order to get a fair prediction of the pressure perturbations originating from rotor movements, a high quality CFD flow solution is first needed for the CROR. The following work is aimed to do just that, by first devising a model with high mesh resolution, both structured and unstructured with varying domain sizes, and later comparing the FLUENT solutions for three such unstructured mesh domains for the CROR.

II. Geometry and Test Case Definition

a) Hub and Blade Geometry

An arbitrary CROR power plant model was used based on the model tested by GE. One generic blade geometry was created using SolidWorks CAD-software, which was then mirrored about its XZ plane to provide the basis for a second row of counter rotating propellers (figure 2). No gas turbine-core was taken into consideration in this analysis as it will further complicate the problem at this time.

Two rotor configurations, varying only in the combination of blades count in the forward and aft rotors, were created consisting of 12x12 and 12x10 blades (figure 3). Both configurations had a forward rotor diameter $d_{fwd} = 68.6in$ and $d_{aft} = 66.6in$ diameter for the aft row. Giving it a mean rotor diameter of $D = 67.6in$, with hub-to-tip ratios of $d_{fwd}/D = 0.201$ and $d_{aft}/D = 0.182$ for the forward and aft rotors respectively. The rotor spacing was arbitrarily chosen as $x/D = 0.235$ and the total length of the hub was taken was *100in* (figure 2).

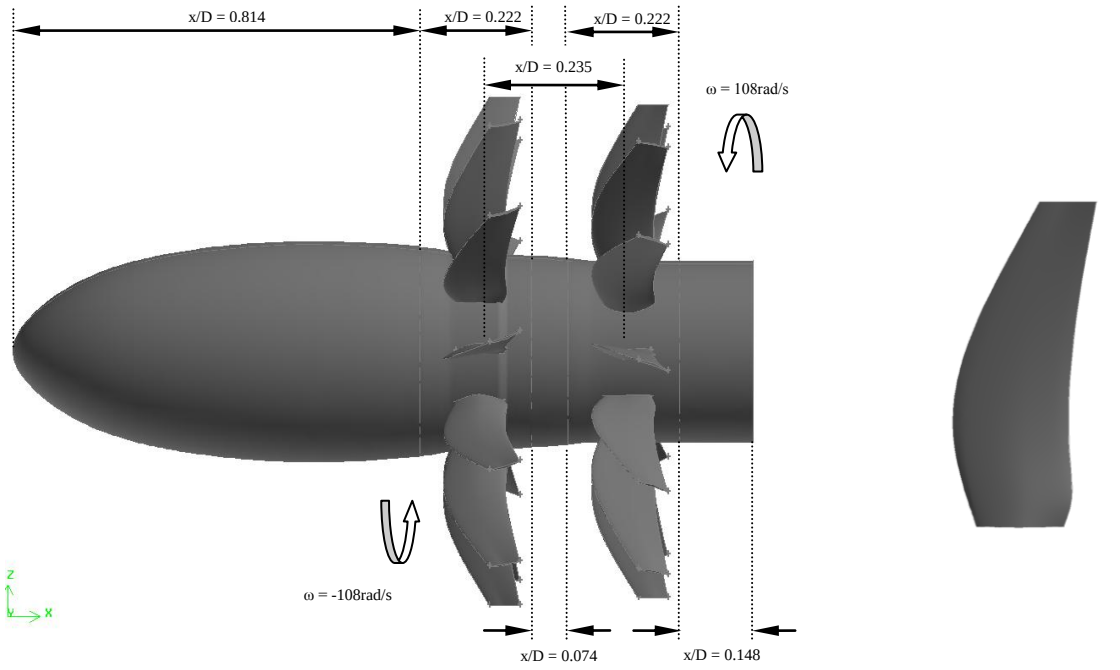

(i) Overall CROR geometry

(ii) Blade geometry

Figure 2: CROR geometry layout

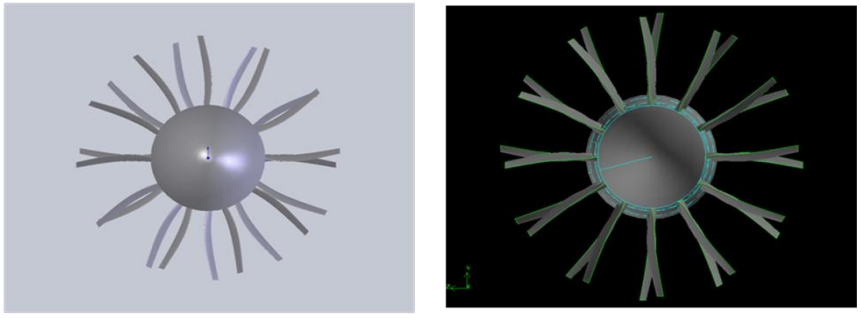

(i) 12x10 blades count

(ii) 12x12 blades count

Figure 3: Rotor configurations

b) Engine Operating Conditions

The operating conditions for the CROR were chosen from Struemer and Yin's[1] paper. Flow speed was set at $V_{in} = 69m/s$ ($M = 0.2$) to simulate a low speed take-off situation at sea-level. The rotational speed for both rotors was set to *1029rpm* (=108*rad/s*), which is equivalent to a mean tip Mach number of *M=0.27* of the blades. Table1 summarizes these conditions:

Table 1: Engine Operating Conditions[1]

		Rotor 1		Rotor 2	
	Configuration	ω_{R1}		ω_{R2}	
Take-off at sea level: *T = 288K* and *M=0.2*					
Config-1	12 x 12	-1029*rpm*	-108*rad/s*	1029*rpm*	108*rad/s*
Config-2	12 x 10	-1029*rpm*	-108*rad/s*	1029*rpm*	108*rad/s*

III. Computational Domain and Meshing Strategies

a) Choice of Mesh Domain

Two types of mesh domains were generated using both structured and unstructured meshing schemes for each configuration. First domain type consisted of mesh for one passage only, which was resolved using periodic boundary conditions at the symmetry faces. The aim for this strategy was to reduce computation time and memory requirements for each case. The passage shape was particularly straight forward in case of 12x12 configurations, as it had no mismatch between the two blade rows. However, in case of the 12x10 configuration, there was a mismatch between the two blade rows as illustrated in figure 4. A combination of rotor-rotor interface boundary conditions was used to account for this mismatch while solving in FLUENT.

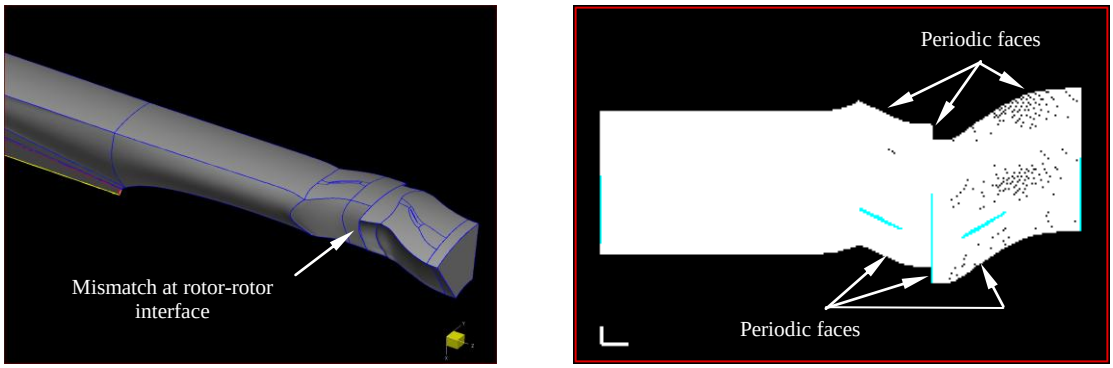

(a) Isometric view (b) Top View

Figure 4: Domain mismatch at the rotor-rotor interface for 12x10 configuration

A second type of mesh domain consisted the whole 360° annulus geometry, with all available passages included. There was no need for a “rotor-rotor interface” in this case, as all external faces were set as either interior or pressure far-field boundaries. However, this choice of domain had particularly increased the number of required mesh elements needed for a decent flow solution, which in turn took considerably more computational power and time to solve for each time-step. Figure 5 illustrates the full-annulus mesh domain for the 12x10 configuration with all passage meshes included in one domain.

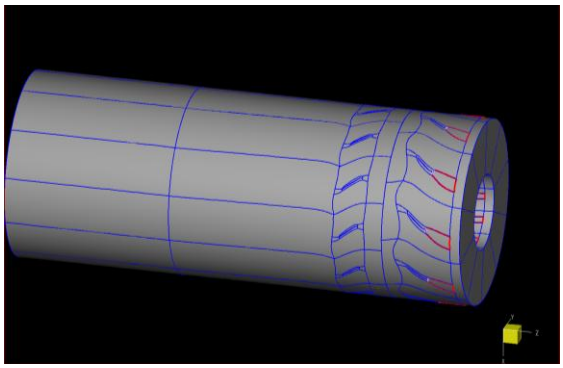

Figure 5: Full-annulus mesh domain for the 12x10 configuration

b) Mesh Generation

Meshing tools available in the FineTurbo® CFD-software suit were used to generate the structured mesh, while GAMBIT® was used for unstructured mesh generation. Special care was taken for meshing the boundary layers near blade walls and regions near the leading (L.E.) and the trailing (T.E.) edges, as these were the most critical areas for a

better solution. A “sleeve” of structured boundary layer (B.L.) mesh was applied surrounding the blade geometry to appropriately resolve the near wall boundary layers close to the blade surfaces (figure 6).

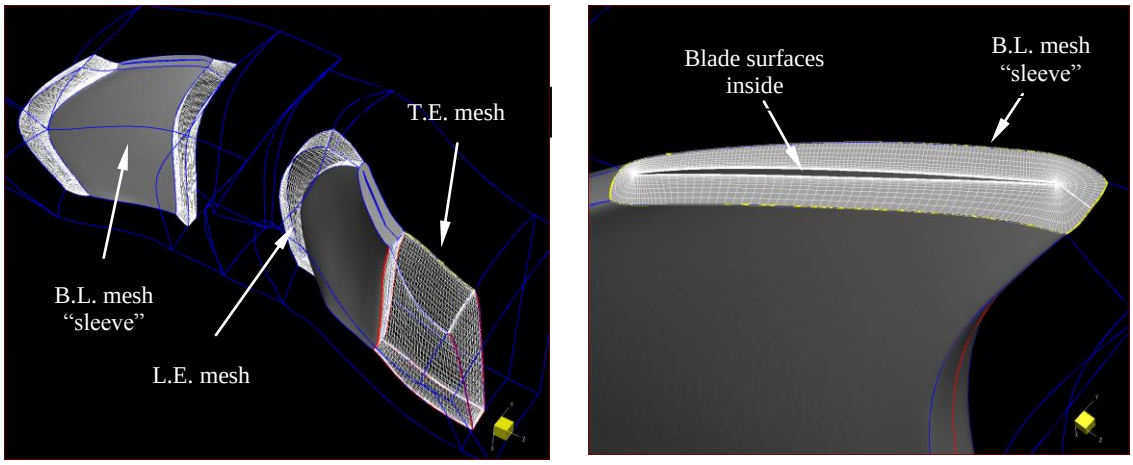

Figure 6: Structured mesh taking into account L.E., T.E. and B.L.

FineTurbo® provides a flexible meshing tool that allows users to manually adjust mesh resolution at the micro-level of any critical area. Similarly, GAMBIT provides its own set of tools to manually adjust mesh resolution at problematic areas such as curves and corners. Meshing with GAMBIT was largely an automated process in that one had to specify only the desired density of elements on a line, face or volume and the mesh was automatically generated. However it did not guarantee a flawless execution every time. For example, in the regions where sharp edges were present in the geometry, there were

often irregular shaped highly skewed mesh elements found which needed to be refined in order to reduce probability of divergence in the FLUENT solver. Hence, in order to obtain a better mesh resolution, nodes were manually redistributed every time at areas where such "highly-skewed" (equisize skew > 0.97) mesh elements were spotted, as illustrated in figures 7 (i) and (ii).

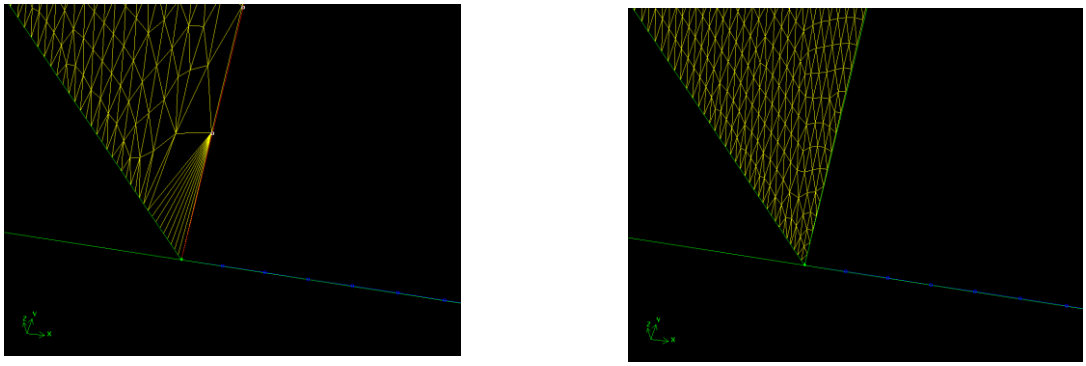

(i) Problematic mesh region (ii) Same region after manual refinement

Figure 7: Development of unstructured mesh

Furthermore, a better resolution face mesh did not always guarantee a well defined volumetric mesh. Whenever a problem was found during volume mesh generation, the whole exercise of line and face meshing needed to be started over again from scratch. After a rigorous trial and error approach, it had been perfected to a stage where the worst element skewness was kept under 0.6 for the 3D elements. The resulting unstructured mesh also included a B.L. region near the surfaces of the blades and a fine tetrahedral tri-mesh region encapsulating the rotors (figures 8 and 9 (i)).

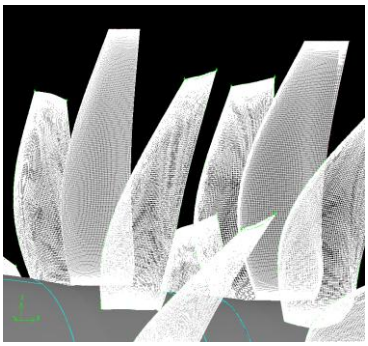

Figure 8: Unstructured B.L. mesh near blade walls

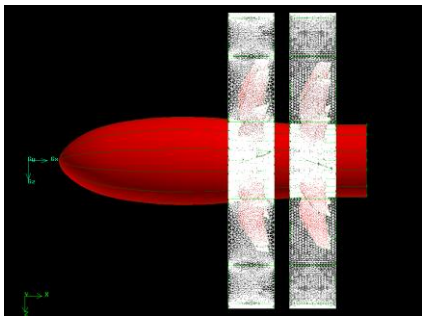

(i) Dense rotor mesh

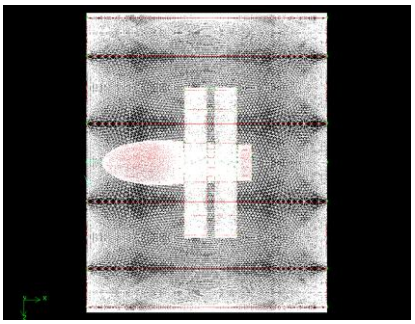

(ii) Denser inner mesh

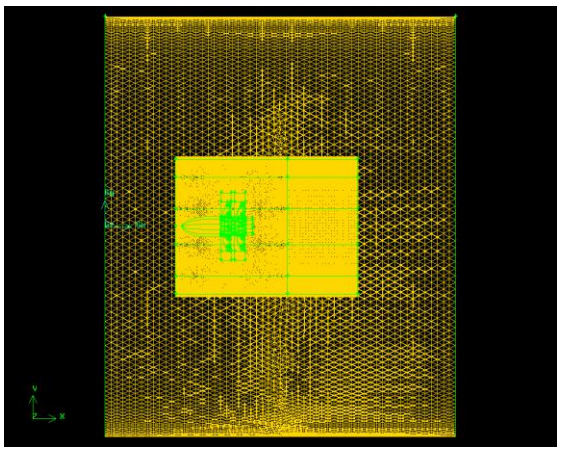

(iii) Coarse outer mesh

Figure 9: Development of unstructured mesh

c) Far-Field Mesh Domain

As this is an open-rotor situation and the flow solution is intended for acoustic analysis in the long run, a far-field mesh domain was also produced. The far-field domain was generated by projecting the top face of the rotor domain radially outwards up to a distance of $d_{ff} / D = 10$. Two such domains had been tested. Struemer[1] used a far-field domain reaching out to $d_{ff} / D \approx 5$. But, to find out how far is far enough for the far-field, a mesh with $d_{ff} / D = 3$ and another with $d_{ff} / D = 10$ was chosen for far-field domain size. Two mesh fields for both single passage and the whole annulus, with different far-field domain sizes (both $d_{ff} / D = 3 \; and \; 10$), were created and tested (figures 9 (ii) and (iii)).

The structured far-field mesh generation was particularly tricky as there needed to be separate mesh blocks to fill in the "void" created by the blade tips after the top face mesh was projected radially outwards. These blocks were constructed from the blade tips to the far-field only (see Figure 10 (v)). Figure 10 summarizes both final structured and unstructured meshes for the current project.

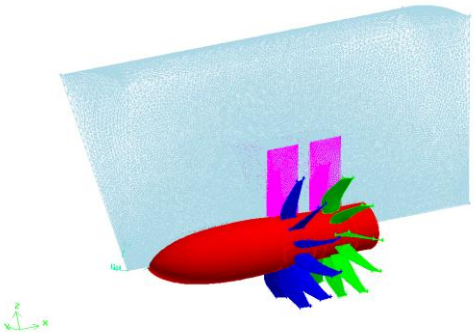

(i) Single passage far-field mesh (unstructured)

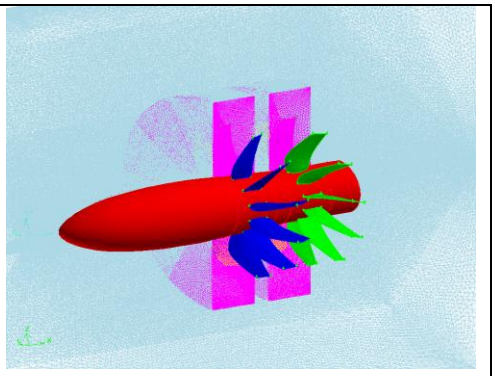

(ii) Full annulus far-field mesh (unstructured)

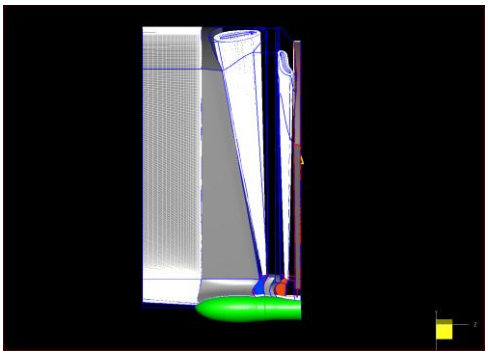

(iii) Single passage far-field mesh (structured)

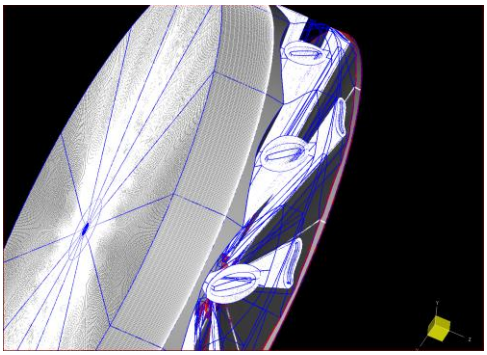

(iv) Full annulus far-field mesh (structured)

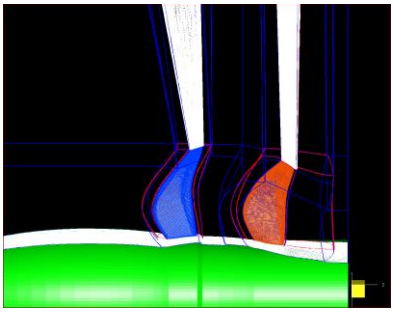

(v) Filling in the tip "voids" for the structured mesh

Figure 10: Far-field mesh generation

IV. Flow-Field Solutions

Flow-field solution was obtained for the unstructured meshes only. Three mesh domains: (i) single passage with periodic BC and far-field $d_{ff} / D = 3$, (ii) full annulus with far-field $d_{ff} / D = 3$, and (iii) full annulus with far-field $d_{ff} / D = 10$ - were run to see if steady state convergence occurred. None of these meshed models converged after running a considerable amount of iterations, in fact, for all three cases the residuals remained roughly the same for more than 50,000 iterations while trying to reach a steady-state solution (figure 11). This was expected for a counter rotating rotor system, where the flow-field was inherently unsteady due to complex rotor-rotor interactions.

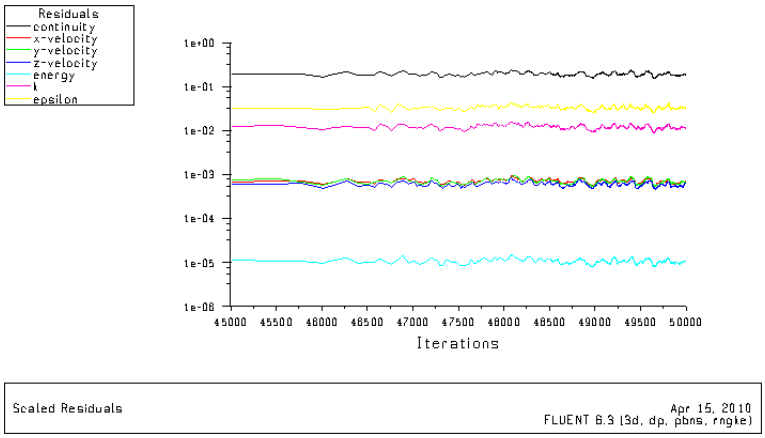

Figure 11: Mesh type (ii) residuals history

Being unable to reach a steady-state solution for a large number of iterations, the solution was then diverted to the FLUENT unsteady solver using the un-converged steady-state

results as the initial conditions. The unsteady solver was run using an 2nd Order implicit method with a very conservative time-step size of $\Delta t = 5 \times 10^{-6}$. The results for the three mesh domains are compared in Table 2 after each was run for 200 time-steps. The first column shows velocity contours at a plane slicing through the middle of the mesh domains. The second column shows the velocity profiles at a particular downstream point **(*x/D* = 1.5)** for all three domains.

Table 2: Comparison of three mesh domain unsteady results

	Mesh Domain	Velocity Contour Plot	Velocity Profile at *x/D = 1.5*
(i)	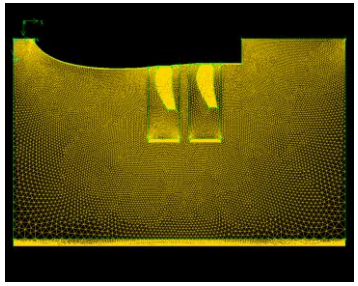 Single passage with periodic BC	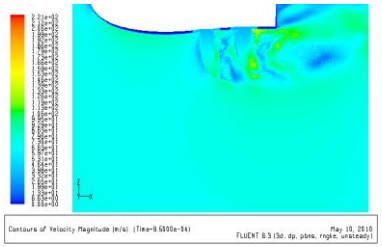	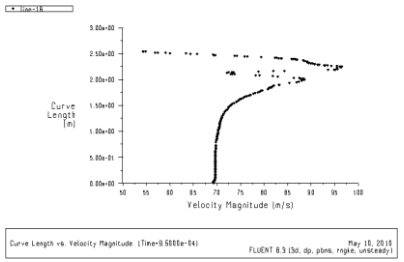
(ii)	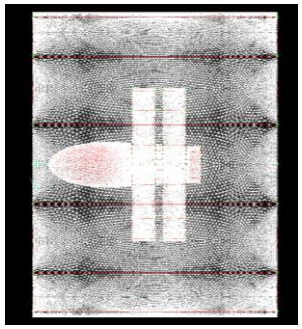 Full annulus with far-field *d/D=3*	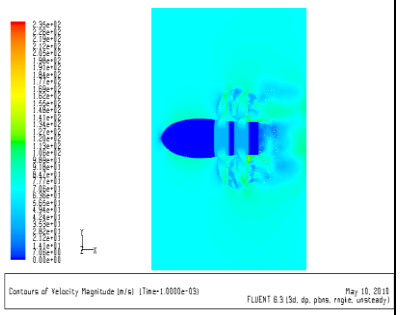	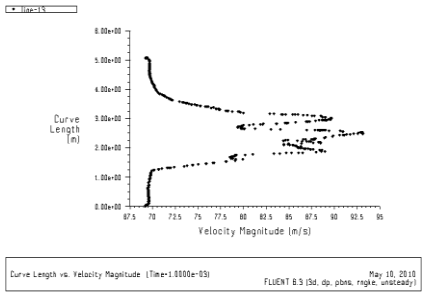
(iii)	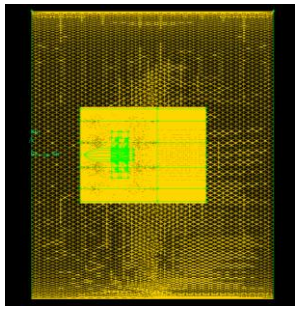 Full annulus with far-field *d/D=10*	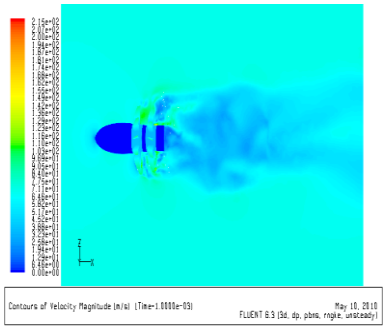	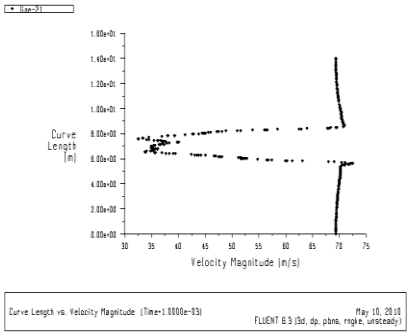

It could easily be seen that none of these plots are exactly the same, although they are taken roughly at the same flow-time. And most of all, the flow was certainly not symmetric, as one could guess by looking at the first case only. However, from the mesh results (i) and (ii), which have the same dimensions except that the first one is a one-twelfth fraction of the second, it is observed that the flow solution is nearly the same. This indicates that one could use only the single passage results to predict the flow properties around the whole annulus without much loss of accuracy. Furthermore, the full annulus results for domains (ii) and (iii) indicates the validity of the large mesh domain ($d_{ff} / D = 10$) as a more suitable flow solution. However, solution of domain (iii) takes a large amount of processing time and effort compared to the other two domains in order to converge at each time-step. Hence, in light of limited computational time and recourses one might face, it is only appropriate to use a single passage mesh with a large far-field domain equal or more than $d_{ff} / D = 10$.

V. Discussion

Figure 13 illustrates the velocity contours and stream vectors are showing the wake regions at the blade trailing edges. In Figure 14, the path-lines at the two rotors show the vorticity and swirl occurring at the wake region.

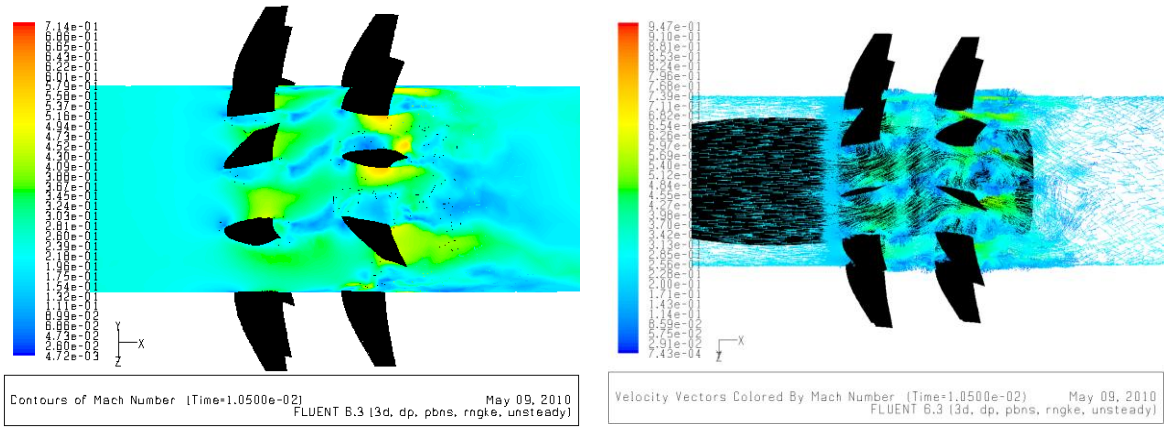

Figure 12: Wake region at the blade trailing edges

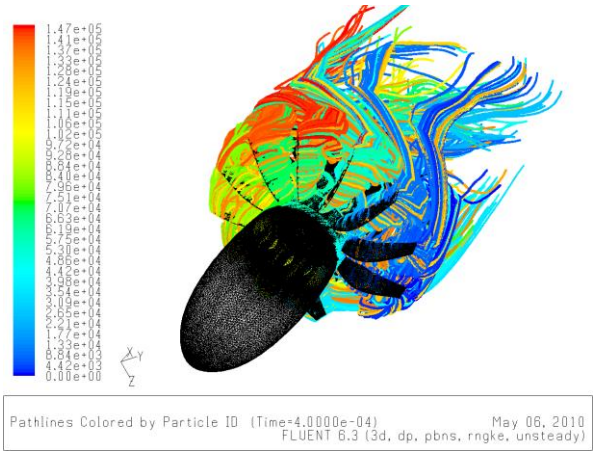

Figure 13: Path-lines showing the swirling flow

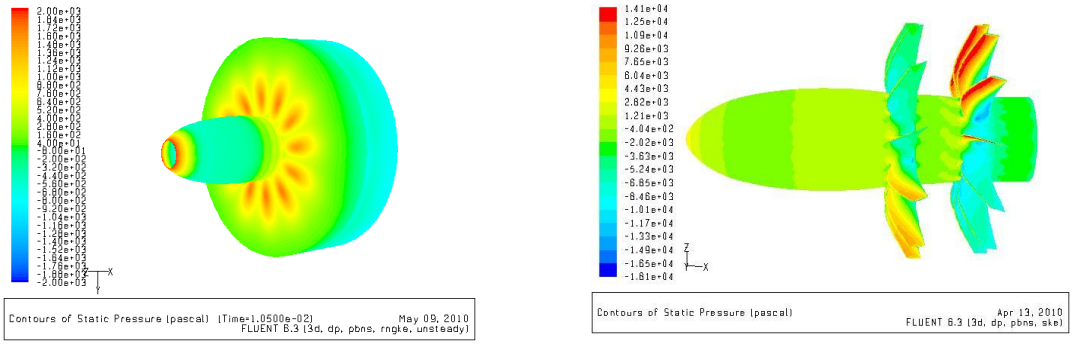

Figure 14: Static pressure plot at the two rotor regions

Figure 15 shows the static pressure plots at the two counter rotating rotors. As expected, static pressure was the highest at the hub's nose and at the blade tip regions. Figure 13 shows the highly turbulent wake region produced by the two rotors, which, in fact, is a major source for aerodynamic noise generation.

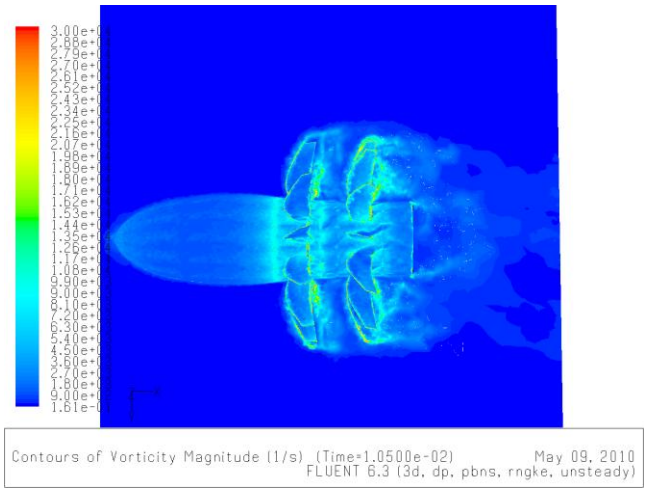

Figure 15: Turbulence at CROR downstream

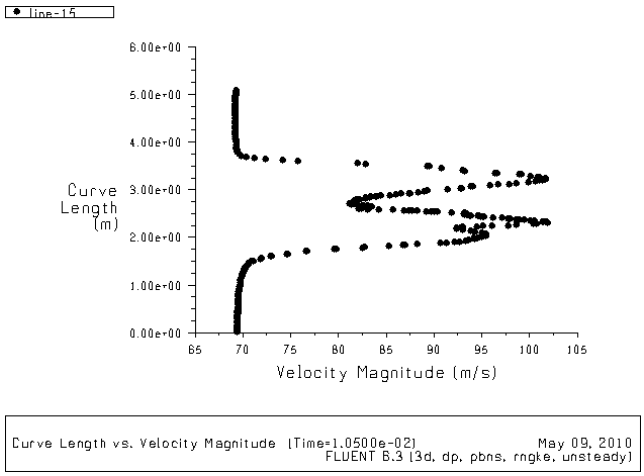

Figure 16: Velocity profile at *x/D =1.5*

Finally, Figure 14 shows the same velocity profile at the same point in Table 2 - case (ii). This profile also demonstrates that the flow had reached a point where the initial disturbances were not present and the flow was also not an axi-symmetric one.

VI. Conclusion

Research efforts have already been made at various academic and industry levels to address the noise issue using the computational aeroacoustic (CAA) approach. CAA is a modern tool that researchers use to deal with direct applications of classical acoustics in the specialty field of aerodynamic noise reduction. For a better performing CAA tool, a good CFD model is always desired. Path has been laid out in this study for a future coupled aerodynamic and aeroacoustic analysis of the CROR engines. The CFD results showed that the most critical region for acoustics purposes is at the two rotors and the wake regions. Flow between the front and aft rotors is of particular interest as there is a subsequent phenomenon of fluid being continually “twisted” and “untwisted” by the counter-rotating front and aft rotors respectively, causing a potent area for waveform fluctuations causing disturbances in the audible range. These areas need to be further investigated in future and examined how and where the noise sources occur. Once a good approximation is obtained, the means for which was the main focus of this paper, the CROR design may be optimized to maximize performance and minimize noise polution.

VII. References

[1] Stuermer & Yin *et al*., "Low-Speed Aerodynamics and Aeroacoustics of CROR Propulsion Systems," AIAA Paper 2009-3134, 2009.

[2] Page, L., *"NASA working on 'open rotor' green (but loud) jets: Want to save the planet? Put up with noisier airports",* http://www.theregister.co.uk/2009/06/12/nasa_open_rotor_trials/

[3] Hussaini, M.Y. & Hardin, J.C., "Computational Aeroacoustics," Springer-Verlag, NY, 1993.

[4] SenGupta, G. *et al*. "Application of computational methods in aeroacoustics," AIAA Paper 90-3917, 13th AIAA Aeroacoustics Conference, Tallahassee, FL, 1990.